

Optical and Transport Anisotropy in Poly(9,9'-dioctyl-fluorene-*alt*-bithiophene) Films Prepared by Floating Film Transfer Method

Arnaud Dauendorffer, Shuichi Nagamatsu¹, Wataru Takashima², and Keiichi Kaneto

Graduate School of Life Science and Systems Engineering, Kyushu Institute of Technology, Kitakyushu 808-0196, Japan

¹Department of Computer Science and Electronics, Kyushu Institute of Technology, Iizuka, Fukuoka 820-8502, Japan

²Research Center for Advanced Eco-fitting Technology, Kyushu Institute of Technology, Kitakyushu 808-0196, Japan

Received December 13, 2011; revised February 8, 2012; accepted March 2, 2012; published online April 19, 2012

We demonstrated the fabrication of self-aligned poly(9,9'-dioctyl-fluorene-*alt*-bithiophene) copolymer (F8T2) thin films at ambient temperature with a new solution-process technique named floating film transfer method (FTM). Atomic force microscope topography and polarized absorption spectroscopy showed that the polymer main chains aligned perpendicularly to the film propagation direction during the fabrication process. FTM films presented absorption dichroic ratios slightly below 3. Top-contact/bottom-gate field effect transistors made with FTM films exhibited anisotropic transport properties with a hole mobility along the aligned direction of F8T2 main chains of $2.2 \times 10^{-3} \text{ cm}^2/(\text{V}\cdot\text{s})$, which was around 2.5 times greater than that along the perpendicular direction. Dichroic and transport anisotropy ratios were further enhanced up to 7–8 by thermal annealing, although the mobility improvement remained limited due to possible trapping effect at domain boundaries.

© 2012 The Japan Society of Applied Physics

1. Introduction

Conjugated polymers represent a promising alternative toward ubiquitous cheap, lightweight and flexible electronics devices such as organic field-effect transistors (OFETs), organic light emitting diodes (OLEDs), and organic solar cells (OSCs).¹ Semiconducting properties of conjugated polymers arise from the electrons delocalized along the backbone structure of the polymers. Higher carrier mobilities and polarized photon emission are thus expected when conjugated polymer films are macroscopically ordered. For this reason, control of polymer ordering during the film forming process has attracted much recent attention and various alignment methods have been developed such as stretch alignment,² dip-coating,³ the Langmuir–Blodgett (LB) technique,⁴ nanoconfinement during nanoimprinting,⁵ thermal annealing on an alignment layer,^{6–10} the friction transfer method,^{11–14} or laser annealing.¹⁵

We invented a new technique to make large-area thin films on a viscous hydrophilic liquid surface. The resulting floating film can then be easily transferred onto a solid substrate by stamping. This method was therefore named floating film transfer method (FTM) and is somehow similar to *Suminagashi* in Japanese painting (or marbling), in which a patterned ink on water surface is transferred onto paper by skimming. The technique is also similar to the LB method although there is no surface-pressure application to make a compact film here. The enhancement of transport properties in poly(3-hexylthiophene) (P3HT) thin-films deposited with this method has been already reported in the literature.¹⁶

Poly(9,9'-dioctylfluorene-*alt*-bithiophene) alternating copolymer, or commonly abbreviated F8T2, presents several favorable properties which make it convenient for studying optical and electrical properties of thin films. The presence of conjugated segments assures efficient charge carrier transport and it presents high luminescence efficiency and a relatively good stability under the atmosphere. Moreover, the presence of two long octyl chains protruding from the rod-like backbone ensures good solvation in various organic solvents (see inset in Fig. 2). It also exhibits a thermotropic nematic liquid crystalline (LC) phase above 265 °C that

can be oriented into a monodomain on an alignment layer by subsequent thermal annealing.⁶ Various research groups have been using this technique to build OFETs with highly oriented F8T2 active layers formed on photoaligned or rubbed alignment layers,^{7–10} resulting in a significant enhancement in the device characteristics with mobilities up to 3 times higher than in isotropic thin films. Other groups reported alignment of F8T2 achieved via the friction-transfer technique,¹³ with even the formation of F8T2 nanowires by Li *et al.*¹⁴ Lately, a new technique based on laser annealing was also proposed.¹⁵

Recently, we discovered a new functionality of the FTM to prepare large-scale (in centimeter order) oriented floating films by using polyfluorene family polymers. It was found that self-aligning LC conjugated polymers like polyfluorene and its derivatives showed a large-area dichroism in FTM films, whereas it was not observed in P3HT films. Hence we decided to investigate this new phenomenon in order to understand its formation mechanism and demonstrate its application to the improvement of transport properties in OFETs. In this report, we present the optical and transport anisotropic properties of one-dimensionally oriented F8T2 thin films prepared by FTM. Thin films were first characterized by polarized absorption spectra and atomic force microscope (AFM) measurements. Then, we fabricated OFETs utilizing oriented FTM thin films and compared them to spin-coated OFETs having the same active layer thickness. Polymer alignment was achieved here without using any special alignment layer or thermal treatment of the substrate, which represents the main advantage of this new technique. This may be particularly interesting for the rapid mass fabrication of plastic based flexible devices which requires low temperature processes. Finally, we briefly discuss the effect of subsequent thermal annealing below the nematic phase transition temperature.

2. Experimental Procedure

F8T2 was synthesized by Suzuki coupling,¹⁷ and stored in ambient conditions. Weight average and number average molecular weights (M_w and M_n , respectively) were determined from tetrahydrofuran solutions by gel permeation chromatography (GPC) using polystyrene equivalents. All results presented here are obtained using a polymer

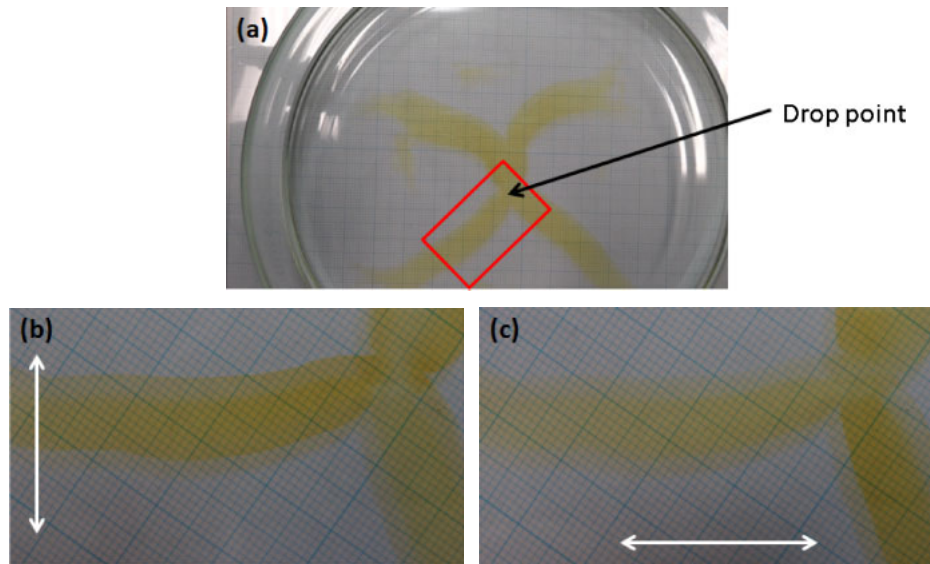


Fig. 1. (Color online) (a) Picture of a F8T2 branched floating film when the solution is dropped at the center of a Petri Dish. (b) Orientation is clearly observed when observing through a linear polarizer. (c) Orientation is switched by rotating the polarizer 90° . The arrows in (b) and (c) indicate the transmission axis of the polarizer.

with $M_w = 39.7$ kg/mol and polydispersity index, $PDI = M_w/M_n = 1.6$. The glass transition temperature and nematic LC transition temperature were found to be $T_g = 67^\circ\text{C}$ and $T_{LC} = 261^\circ\text{C}$, respectively, from DSC measurements (Shimadzu DSC-60). These values are comparable to those measured by other groups.^{8,13,15}

F8T2 films were prepared on glass substrates and highly p-doped silicon wafer with 100-nm-thick SiO_2 by the FTM transfer method. A 10 mg/mL F8T2 solution dissolved in dried chloroform was prepared and filtered through a $0.2\ \mu\text{m}$ poly(tetrafluoroethylene) (PTFE) filter. Then, a drop of solution (approximately $25\ \mu\text{L}$) was deposited with a microsyringe on ethylene glycol poured in a Petri dish and kept at 25°C . The solution being hydrophobic, it spread over the ethylene glycol surface, forming a floating thin on the liquid surface. In case of F8T2, a branched floating film was formed (Fig. 1). By seeing the film through a polarizer, the branched film appeared oriented concentrically with the drop point as center. In order to form a uniformly oriented large film, the solution was dropped from the edge of the Petri dish, resulting in a unidirectional propagation of a branch free film. Part of this floating film was then transferred onto a substrate by first making the substrate surface lightly touch on the floating film, and then carefully lifting it up. Spin-coated films were also prepared for comparison. A 5 mg/mL F8T2/chloroform solution filtered through a $0.2\ \mu\text{m}$ PTFE filter was used to make spin-coated films having a similar thickness to FTM films. The thicknesses of all the films were within 30–35 nm, measured by a Dektak profilometer.

Optical properties of both types of thin films were assessed by polarized UV–visible absorption spectra using a JASCO V-570 spectrophotometer with a Glan Thomson polarizing prism. Surface topographies were investigated with an AFM equipment (JEOL SPM5200). All the images were obtained via tapping mode with probes purchased from Olympus (OMCL-AC200TSC3).

Electrical properties of the films were assessed by the fabrication of OFETs having a top-contact/bottom gate structure. As mentioned above, a highly p-doped silicon wafer with a 100-nm-thick SiO_2 insulating layer was used as substrate and gate electrode. The SiO_2 thickness provided a capacitance per area of $30\ \text{nF}/\text{cm}^2$. The substrates were then hydrated with aqueous ammonia and hydrogen peroxide followed by silanization with octyltrichlorosilane (OTS) to form a strong hydrophobic surface.¹⁸ Thin films were then coated in ambient atmosphere by FTM or spin-coating. Finally, two gold electrodes (40 nm thick) were deposited on the F8T2 films at $\sim 10^{-4}$ Pa by vacuum evaporation using a shadow mask to form the top contact source/drain electrodes. The channel length (L) and width (W) were $20\ \mu\text{m}$ and 2 mm, respectively. All devices were temporally exposed to air prior characterization by a two channel electrometer (Keithley 2612). Drain current–drain voltage ($I_{\text{DS}}-V_{\text{DS}}$) as well as the drain current–gate voltage ($I_{\text{DS}}-V_{\text{GS}}$) characteristics were measured under vacuum at $\sim 10^{-4}$ Pa. Field effect mobility, μ , and the threshold voltage, V_{th} , were extracted from the transfer characteristics at the saturated regime in $(\sqrt{I_{\text{DS}}-V_{\text{GS}}})$.¹⁹

3. Results

Figure 1(a) presents a F8T2 branched floating film made by FTM. By observing the FTM film through a linear polarizer, we easily noticed with the naked-eye that the intensity of the film color changed when rotating the polarizer. The material color was highlighted in the area where the propagation direction of the film was perpendicular to the transmission axis of the polarizer [Fig. 1(b)]. This was clearly switched by rotating the polarizer 90° [Fig. 1(c)]. According to this observation, the polymer chains were clearly self-aligned perpendicularly to the propagation direction over a long distance of several centimeters during the FTM film formation.

The degree of alignment can be quantified from the polarized optical absorption spectra. Figure 2 presents

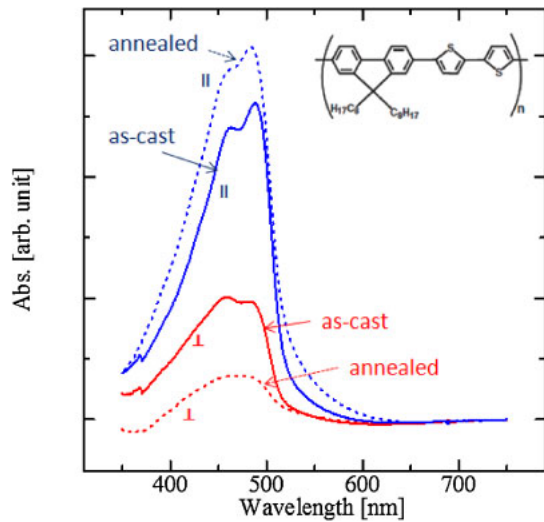
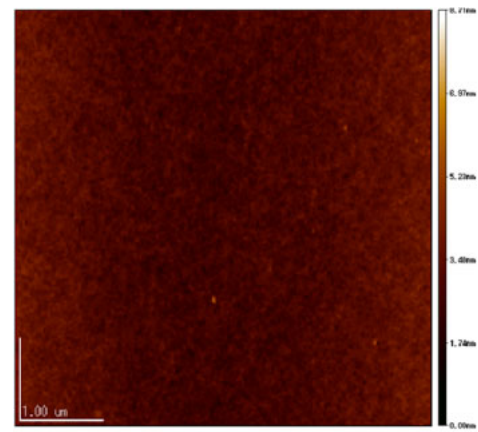


Fig. 2. (Color online) Polarized absorption spectra of a FTM film before and after annealing (||: prism parallel to the main chain orientation, ⊥: prism perpendicular to the main chain orientation). Chemical structure of F8T2 is also presented in inset.

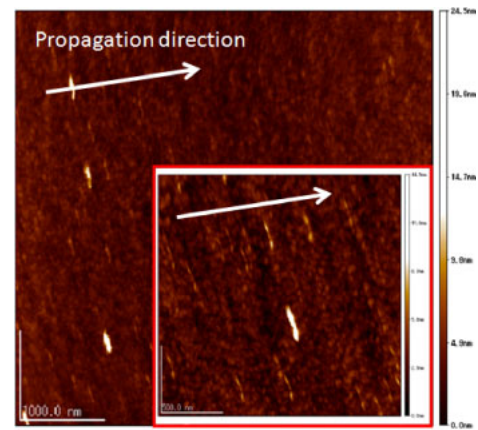
polarized absorption spectra of a 30–35 nm thick F8T2 FTM film transferred on a glass substrate. Here, we define the absorption spectra in parallel and perpendicular to the polymer alignment direction as $A_{||}$ and A_{\perp} respectively. The strong absorption in the wavelength region from 350 to 550 nm corresponds to the π - π^* transitions on the F8T2 backbone, which is polarized along the backbone structure.⁷⁾ The dichroic ratios $A_{||}/A_{\perp}$ at the absorption maxima of 462 and 489 nm were 2.4 and 2.8 respectively. These values are a bit lower than in films made with other methods (between 6 and 12).^{7–10,13)} However, it is important to remind that, contrary to other methods, FTM films were made at ambient temperature and present natural alignment without need of post-treatment or mechanical stress.

AFM images of thin films deposited by spin-coating and FTM on flat silicon wafer substrates are presented in Fig. 3. The spin-coated film shows a relative flat surface ($R_q = 0.348$ nm) with a fine particle like structure [Fig. 3(a)]. This suggests that an amorphous like polymer uniformly covered the surface. On the other side, the FTM film presents a slightly coarse surface ($R_q = 1.14$ nm) which consists of fibrous like domains [Fig. 3(b)]. As we can see in the magnified picture in inset, these domains appear to be aligned perpendicularly to the propagation direction, which is consistent with the polarized absorption.

FTM films were also annealed at 190 °C during 30 min in Argon gas. This temperature was initially chosen so as to remove possible remains of ethylene glycol from inside the films. Interestingly, the dichroic ratio got improved and reached values between 8 and 9. These ratios are similar to the values obtained by other groups and their respective methods.^{7–10,13)} Figure 2 presents the absorption spectra of a FTM film before and after annealing. Optical anisotropy got improved by an increase of absorption in the parallel direction and a drop in the perpendicular direction, indicating the enhancement of the uniaxial alignment of the polymer. The annealing temperature used



(a)



(b)

Fig. 3. (Color online) (a) AFM image of an as-cast spin coated film ($5 \times 5 \mu\text{m}^2$). (b) AFM image of an as-cast FTM film ($5 \times 5 \mu\text{m}^2$) with a magnified image in the inset ($2 \times 2 \mu\text{m}^2$).

here was below the nematic LC transition but over the glass transition temperature of F8T2. This temperature might act as a driving force to homogenize the orientation of misoriented chains along the orientation achieved by FTM.

In order to investigate the relationship between structural and electrical properties of FTM films, top-contact/bottom gate OFETs were fabricated. Two orientations of the channel were used to build devices with the channel direction parallel and perpendicular to the polymer orientation (Fig. 4). Hereafter, we represent the former devices “parallel OFETs” and the latter devices “perpendicular OFETs”. These two types of devices were assessed from the same floating film. We first examined the transport properties of as-cast F8T2 thin films made by FTM. Spin-coated films having a similar thickness were also built for comparison. Experiments were repeated several times in the same conditions and similar results were obtained. Typical transfer characteristics are presented in Fig. 5(a) and the corresponding OFET parameters are summarized in Table I. Both OFETs fabricated with FTM and spin-coated films exhibited clear normally-off transistor behavior. Parallel devices were found to exhibit higher mobilities than perpendicular devices, with a field-effect mobility ratio $\mu_{||}/\mu_{\perp}$ between 2.5 and 2.7, depending on FTM films. Mobilities of

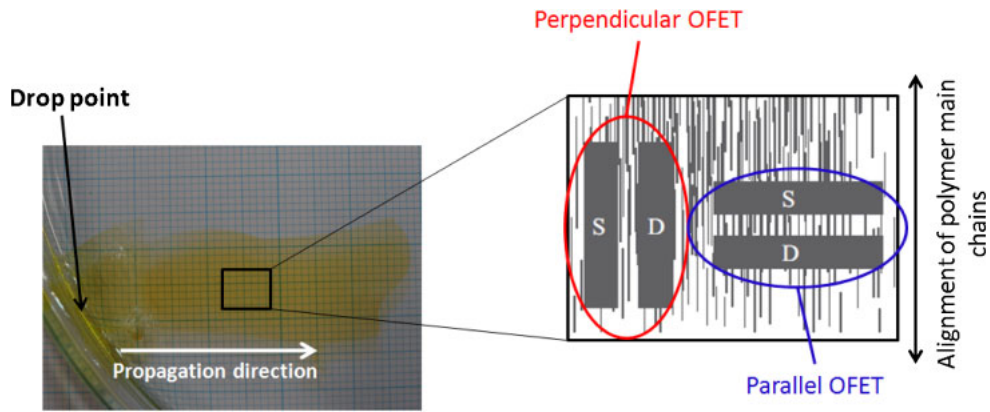


Fig. 4. (Color online) Schematic representation of the channel orientation for oriented FTM thin films OFETs.

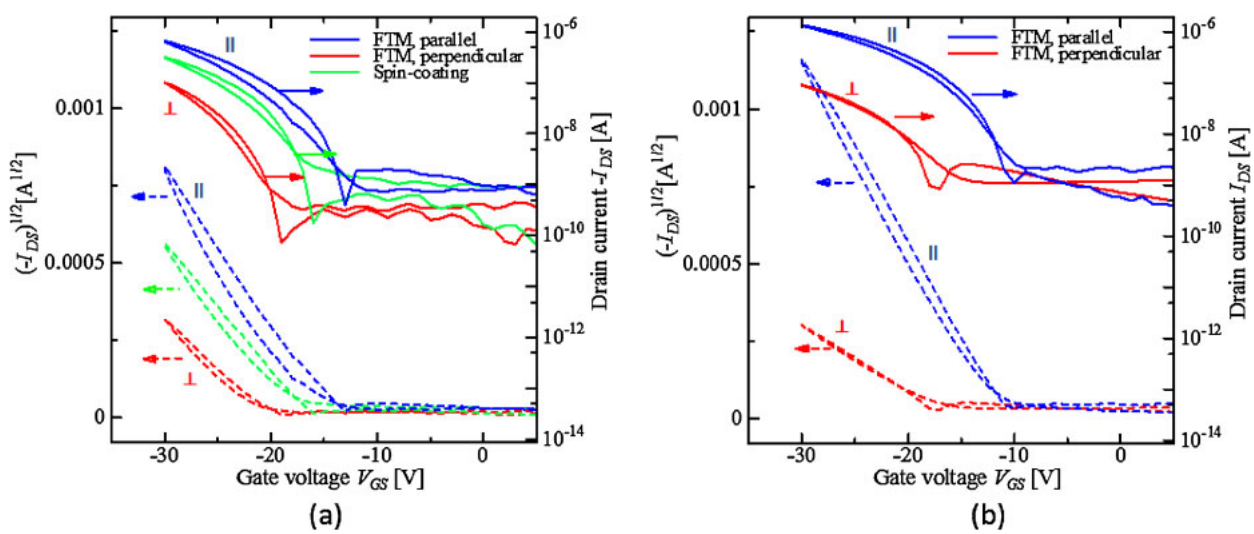


Fig. 5. (Color online) Typical transfer characteristics of OFETs made with as-cast F8T2 thin films (a) and annealed thin films (b).

Table I. Typical FET parameters in OFETs for FTM and spin coated thin films.

	FTM parallel	Spin coating	FTM perpendicular
As cast			
V_{th} (V)	-16	-17	-21
μ [$\text{cm}^2/(\text{V}\cdot\text{s})$]	2.2×10^{-3}	1.2×10^{-3}	8.2×10^{-4}
ON/OFF ratio	770	440	350
Thermal annealing			
V_{th} (V)	-11	-15	-16
μ [$\text{cm}^2/(\text{V}\cdot\text{s})$]	2.6×10^{-3}	2.2×10^{-4}	3.3×10^{-4}
ON/OFF ratio	900	60	100

as cast spin-coated OFETs were found to be in-between parallel and perpendicular FTM devices with $\mu_{\perp} < \mu_{\text{spin}} < \mu_{\parallel}$. This result is reasonable since spin-coating films are isotropic and is in agreement with data obtained by other groups.⁷⁾

We then finally assessed the transport properties of annealed FTM films. Experiments were repeated several times and typical transfer characteristics of parallel and perpendicular devices are presented in Fig. 5(b) with the corresponding OFET parameters being summarized in Table I. As observed in optical measurements, transport

anisotropy in annealed FTM films got improved, reaching mobility ratios between 7 and 8. However, we noticed that this improved anisotropy was mainly due to a decrease in μ_{\perp} , whereas μ_{\parallel} only slightly increased. Transport characteristics in spin-coated films also largely decreased upon annealing with measured mobilities even lower than μ_{\perp} of annealed FTM film.

4. Discussion

First, we discuss the orientation mechanism which occurs during the film formation of FTM. We presume that the apparition of anisotropy is controlled by the balance between the resistive force due to the friction of solidified parts and the driving force coming from the solution propagation on the liquid surface. When a dilute solution (typically less than 5 mg/mL) is used, it spreads quickly over the whole surface of ethylene glycol (or from the edge of the dish). Solidification then starts from the edge of the dish, forming flake like floating regions that will gradually gather to form a large floating film. However, such films do not present any orientation characteristics. On the other hand, when a more concentrated solution is used (like in this study), solidification of the films starts right after dropping the solution. The

region behind the solidification front presents thus higher concentrations which should enhance intermolecular interaction. This continuous solidification should induce the formation of fibrous like structures. The mechanical stacking of features having such high-aspect ratio may provide the perpendicular orientation of these domains as result of the surface stress created by the propagation flow (balance between friction and driving force). This effect could be in a way similar to the LB method where surface-pressure is applied on floating polymer chains to form a floating film. However, in FTM no such external force is applied and we observe a self-organization of the film over a viscous liquid surface. Another candidate for the orientation mechanism could be the formation of lyotropic like LC phase induced by the continuous solidification.²⁰⁾ We have already tried to prepare such oriented films with P3HT, poly(3,3'-didodecyl quaterthiophene) (PQT-12), poly(9,9-dioctylfluorene) (PFO), and various polyfluorene copolymers. As results, PQT-12 and polyfluorenes successfully provided oriented FTM films (results will be published separately), while P3HT failed to provide such clear orientation at the present stage. The reason behind these two different behaviors remains unclear. However, it should be noted that PQT-12 and polyfluorenes are well known for having clear thermotropic LC phase transition behaviors with thermal and optical analysis reported by many researchers,^{21,22)} whereas the LC characteristics of P3HT have not been well defined. Concerning the formation of orientation in FTM, there is no clear evidence to support which mechanism (fibrous structure or LC phase formation) is dominating. Anyway, both the solidification speed and the solution propagation speed are believed to control the orientation formation. The concentration of solution, the solvent, the viscosity and the temperature of the liquid substrate will be the key parameters to control the anisotropy of the films. A careful investigation of different materials may help finding similarities and thus clarifying the mechanism leading to the formation of orientation.

Transport anisotropy in F8T2 FTM films was found to be about the same order as optical anisotropy. Siringhaus *et al.*⁷⁾ proposed a simple geometrical model predicting the mobility anisotropy to be the same order as the dichroic ratio. They also pointed out the limitations of this simple model explaining why measured mobility anisotropies tend to be somewhat lower than optical anisotropies. Transport anisotropy in FTM films shows that charge transport preferably occurs along the polymer chains and is thus faster than hopping from one chain to another. However, it is important to note that the channel length is much larger than the typical persistence length of polymer chains L_p , which is the characteristic length of a straight chain segment. Grell *et al.*²³⁾ determined a value of $L_p \sim 8.5$ nm for the structurally similar PFO. Therefore, even in devices with parallel orientation, interchain hopping dominates and limits the transport rate of the carriers. The mobility ratios obtained here are comparable but somewhat lower to other methods.^{7-10,13,15)} The field-effect mobility measured in our parallel devices is comparable to results obtained by other groups with the same OFET configuration.^{8,13,15)} Higher mobilities were reported by some groups.^{7,10)} However the device structure used was

different (top gate/bottom contact), which prevents a pure comparison of transport performance as also demonstrated by Fujiwara *et al.*⁹⁾

Finally, the effect of annealing on transport characteristics of F8T2 thin films may be considered with the possible role of domain boundaries on device performance. The temperature used here was below the LC transition temperature. Therefore, annealed F8T2 thin films are expected to be in a crystalline phase. Although higher mobilities should be expected due to the presence of crystalline domains, only a slight improvement in parallel FTM OFETs was observed while perpendicular FTM OFETs and spin-coated OFETs presented a large drop of performance. Several groups also reported a similar decrease of hole mobility,^{24,25)} or only a marginal increase,²⁶⁾ after annealing spin-coated F8T2 thin films in the crystalline phase. Newsome *et al.*²⁶⁾ proposed that interfaces between crystalline domains and cluster formations may act to hinder the charge transport and integrity of the interface to the insulator due to an increase of morphology. Mobility decrease upon annealing was also reported in P3HT thin films and attributed to the formation of well define domain boundaries which may act as charge traps.²⁷⁾ On the other hand, F8T2 thin films annealed over the nematic LC phase transition temperature were reported to present enhanced mobilities.^{7,8)} Siringhaus *et al.*⁷⁾ proposed that the glassy LC domain boundaries did not act as traps to the same extent as microcrystalline domain boundaries. These observations highlight the possible role of domain boundaries on the device mobility. A detailed study of the effect of annealing on the film morphology and its influence on device performance is though necessary to confirm the suggested explanations and will be the subject of a future study.

5. Conclusions

In conclusion, we demonstrated that the floating film transfer method (FTM) could provide large-scale uniaxially-oriented film by using poly(9,9'-dioctyl-fluorene-*alt*-bithiophene) (F8T2). Clear optical and transport anisotropy could be observed. AFM measurements showed the alignment of fibrous like domains perpendicularly to the propagation direction. As cast FTM films presented dichroic ratios slightly below 3 at the absorption maxima. The OFETs made with aligned F8T2 films presented hole field-effect mobilities about 2.5 higher along the polymer chain orientation than that of the perpendicular direction. The orientation mechanism during the film formation was discussed with the solidification and the propagation effect. Anisotropy values could be further enhanced by a factor of 3 upon annealing below the nematic liquid crystalline phase transition temperature, although mobility gain in parallel devices was not consequent due to a possible charge trapping effect at domain boundaries.

Acknowledgements

The authors express their thanks to the Center for Microelectronic Systems, Kyushu Institute of Technology, for fabricating Si:SiO₂ substrates. This work was financially supported by an Accelerating Utilization Program of University Intellectual Property from the Japan Science and Technology Agency (JST).

- 1) S. R. Forrest: *Nature* **428** (2004) 911.
- 2) P. Dyreklev, G. Gustafsson, O. Ingnas, and H. Stubbs: *Solid State Commun.* **82** (1992) 317.
- 3) H. N. Tsao, D. Cho, J. W. Andreasen, A. Rouhanipour, D. W. Breiby, W. Pisula, and K. Mullen: *Adv. Mater. (Weinheim, Ger.)* **21** (2009) 209.
- 4) H. G. O. Sandberg, G. L. Frey, M. N. Shkunov, H. Sirringhaus, R. H. Friend, M. M. Nielsen, and C. Kumpf: *Langmuir* **18** (2002) 10176.
- 5) Z. Zheng, K.-H. Yim, M. S. M. Saifullah, M. E. Welland, R. H. Friend, J.-S. Kim, and W. T. S. Huck: *Nano Lett.* **7** (2007) 987.
- 6) M. Grell, M. Redecker, K. S. Whitehead, D. D. C. Bradley, M. Inbasekaran, E. P. Woo, and W. Wu: *Liq. Cryst.* **26** (1999) 1403.
- 7) H. Sirringhaus, R. J. Wilson, R. H. Friend, M. Inbasekaran, W. Wu, E. P. Woo, M. Grell, and D. D. C. Bradley: *Appl. Phys. Lett.* **77** (2000) 406.
- 8) L. Kinder, J. Kanicki, and P. Petroff: *Synth. Met.* **146** (2004) 181.
- 9) T. Fujiwara, J. Locklin, and Z. Bao: *Appl. Phys. Lett.* **90** (2007) 232108.
- 10) K. Sakamoto, T. Yasuda, K. Miki, M. Chikamatsu, and R. Azumi: *J. Appl. Phys.* **109** (2011) 013702.
- 11) S. Nagamatsu, W. Takashima, K. Kaneto, Y. Yoshida, N. Tanigaki, and K. Yase: *Appl. Phys. Lett.* **84** (2004) 4608.
- 12) M. Misaki, Y. Ueda, S. Nagamatsu, Y. Yoshida, N. Tanigaki, and K. Yase: *Macromolecules* **37** (2004) 6926.
- 13) Y. Koshiba, T. Kato, M. Misaki, K. Ishida, M. Torii, T. Kato, K. Tsutsui, N. Tanigaki, K. Yase, and Y. Ueda: *Jpn. J. Appl. Phys.* **49** (2010) 01AE13.
- 14) S. P. Li, C. J. Newsome, D. M. Russell, T. Kugler, M. Ishida, and T. Shimoda: *Appl. Phys. Lett.* **87** (2005) 062101.
- 15) K. Kubota, T. Kato, and C. Adachi: *Appl. Phys. Lett.* **95** (2009) 073303.
- 16) T. Morita, V. Singh, S. Nagamatsu, S. Oku, W. Takashima, and K. Kaneto: *Appl. Phys. Express* **2** (2009) 111502.
- 17) E. Lim, B. J. Jung, and H. K. Shim: *Macromolecules* **36** (2003) 4288.
- 18) S. Grecu, M. Roggenbuck, A. Optiz, and W. Brütting: *Org. Electron.* **7** (2006) 276.
- 19) K. Kaneto, W. Y. Lim, W. Takashima, T. Endo, and M. Rikukawa: *Jpn. J. Appl. Phys.* **39** (2000) L872.
- 20) M. S. Park, A. Aiyar, J. O. Park, E. Reichmanis, and M. Srinivasarao: *J. Am. Chem. Soc.* **133** (2011) 7244.
- 21) S.-H. Yang and C.-S. Hsu: *J. Polym. Sci., Part A* **47** (2009) 2713.
- 22) D. Neher: *Macromol. Rapid Commun.* **22** (2001) 1365.
- 23) M. Grell, D. D. C. Bradley, X. Long, T. Chamberlain, M. Inbasekaran, E. P. Woo, and M. Soliman: *Acta Polym.* **49** (1998) 439.
- 24) K. Koiwai, H. Kajii, and Y. Ohmori: *Synth. Met.* **161** (2011) 2107.
- 25) X. Wang, K. Wasapinyokul, W. D. Tan, R. Rawcliffe, A. J. Campbell, and D. D. C. Bradley: *J. Appl. Phys.* **107** (2010) 024509.
- 26) C. Newsome, T. Kawase, T. Shimoda, and D. J. Brennan: *Proc. SPIE* **5217** (2003) 16.
- 27) D. Choi, S. Jin, Y. Lee, S. H. Kim, D. S. Chung, K. Hong, C. Yang, J. Jung, J. K. Kim, M. Ree, and C. E. Park: *Appl. Mater. Interfaces* **2** (2010) 48.